Chapter 6 Characteristics of Field Emission Triode

6.1 Planar Gated Field Emission Triode

6.1.1 Structural and Electrical Analysis

A low magnification SEM image of the fabricated 2×2 ZnO based triode array is shown in the inset of Fig. 6.1, indicating that the cathode active region is a square opening of 100×100 μm^2, and the distance between the two active regions is 500 μm. The ZnO NWs are successfully and selectively grown inside the gate hole with ZnO seeding areas, but no NWs and other impurities are grown on the gate regions. Figure 6.1 is the enlarged image of the triode device, in which well-aligned ZnO NWs with an average diameter of 50 nm and a number density of 3.4×10^{10} cm^{-2}. These ZnO NWs are randomly oriented, uniformly and selectively grown on ZnO seeding layers inside the cathode active regions. The cross sectional SEM image of ZnO NWs on the substrate is shown in Fig. 6.1(b), indicating that the ZnO NWs were directly grown on the substrate with average length of 500 nm. The polycrystalline ZnO seeding film with the distinct orientation results in the nonvertical random distribution of ZnO NWs.

Figure 6.2 (a) shows the XRD pattern of the ZnO NWs of the field emission triode. The peaks at 33.08^o and 38.5^o in the XRD patterns are caused by the Si substrate and Al metal gate, respectively. The crystal structure of these ZnO NWs is wurtzite and no other phases appear. The lattice constants calculated from the XRD patterns of hydrothermally grown ZnO NWs are a = b = 3.25 Å and c = 5.21Å, which are consistent with that recorded in ICDD No. 80-0074. The HR-TEM image and the corresponding selected area electron diffraction (SAED) pattern of hydrothermally grown ZnO NWs are shown in Fig. 6.2 (b), illustrating the growth orientation and

crystal structure of the NWs. As shown in the figure, the ZnO NWs grew uniformly along [002] direction and the distance between parallel [002] lattice fringes of the ZnO NW is 5.21 Å. The SAED pattern indexed in Fig. 6.2(b) shows that the ZnO nanowire is a single crystalline structure. The lattice constants calculated from the indexed pattern are a = b = 3.25 Å and c = 5.21 Å, which are consistent with those calculated from the XRD result.

The emission current density (J) versus gate bias (V_g) characteristic plots at various applied electric fields (E_a) are shown in Fig. 6.3(a), indicating that a controllable behavior could be divided into three parts: gate leakage region, linear region and saturation region. After the E_a becomes larger than the threshold electric field, the electrons can emit from ZnO NW emitters without applying V_g. Then, the J decreases with an increase in V_g in the gate leakage region. With an increase of V_g from 0 V, the electric field gradient near the ZnO NW emitters will increase due to the short emitter-gate spacing, and consequently some emitted electrons might be trapped by the gate under the gate leakage region which results in the lowering of J., The emission current density in the gate leakage region is decreasing as the gate bias increases since there are more electrons trapped by the gate. As the V_g is continuously increased up to 14 V, the J abruptly increases at linear region. The linear intercept on V_g axis is defined as threshold gate voltage of the linear region, V_{gth}. It is believed that, the induced electric field gradient in the linear region is large enough to accelerate the electrons; consequently, the emitting electrons gain the momentum while passing through the gate to the anode without being trapped. Finally, the field emission current density is saturated as the V_g is larger than 18 V. The high emission current of the triode operated in saturating region may be due to the short gate-tip spacing, small gate aperture and high aspect ratio of the ZnO NWs. The J saturates in the saturating region is owing to the space charge effect of the semiconductor emitters.[189] Here, the

gate leakage region is defined as the field emission off region and the saturation region is the on region. Then, the on/off current density ratio of this field emission triode is about 10^2 under the anode electric field of 2.2 V/μm.

The field emission characteristics can also be observed in the variation of small single transconductance (g_m). Figure 6.3 (b) depicts the relationships between g_m and V_g of the ZnO NW-based field emission triode. The g_m is expressed as the following:

$$g_m = \left.\frac{dI_e}{dV_g}\right|_{V_a} \qquad [6.1]$$

It is to be noted that the g_m is nearly zero below V_{gth} because the I_e is very small at the gate leakage region. The g_m increases in the linear region, goes through a maximum at the point of inflection of linear region to saturation region in the J-V_g curve, and then decreases in the saturating region. The ZnO NW based triode exhibits a high g_m of 2.2 μS under the applied electric field of 2.2 V/μm and a low operating gate bias of 17 V which is the optimized operation voltage of the field emission triode. The μ is an another parameter to evaluate the ability of gate voltage on the emission current density, according to the anode voltage (V_a) and the gate voltage (V_g), which is expressed as,

$$\mu = \left.\frac{dV_a}{dV_g}\right|_{I} \qquad [6.2]$$

From Fig. 6.3 (a), μ is about 100 under the current density of 2 mA/cm^2. Although this μ value is smaller than that (μ=250) of a triode based on plasma-enhanced chemical vapor deposition diamond film, but the low temperature (75 ^{o}C) synthesized ZnO NWs is the first time to be used in the fabrication of the field emission triode device with the controllable ability.

The relationship between J and E_a of the ZnO NW-based triode for different V_g is shown in Fig. 6.3 (c). The turn on electric field (E_{on}, current density of 1.0 μA/cm^2)

and threshold electric field (E_{th}, current density of 1.0 mA/cm^2) are 1.6 and 2.1 V/μm under the zero gate bias, respectively. As the V_g increases to 10 V, the J is depressed to 36 μA/cm^2 under the E_a of 2.2 V/μm. While the V_g increases to 18 V, the E_{th} slightly decreases to 2.0 V/μm but the J abruptly increases to 12 mA/cm^2 under the E_a of 2.2 V/μm. The corresponding F–N plots [ln(J/E^2) vs. E^{-1}] of the ZnO NW-based triode are depicted in the inset of Fig. 6.3(c), indicating that the measured field emission characteristics fit the F–N relationship. The F–N relationship is as the following:

$$J = \frac{A\beta^2 E^2}{\phi}\exp\left(\frac{-B\phi^{3/2}}{\beta E}\right) \qquad [6.3]$$

Where J is the current density, E the applied field, Φ the work function of the ZnO (5.37 eV), β the field enhancement factor, $A = 1.56\times10^{-10}$ (AV^{-2} eV) and $B = 6.83\times10^{3}$ ($VeV^{-3/2}$ μm^{-1}).[136] Thus, the value of β can be calculated from the slope of the *F-N* plot. As shown in the figure, the *F-N* plot under a V_g of 10 V is deviated from the *F-N* fitting, and that under V_g of 0 and 18 V are obeying the relationship with the same slope. The calculated β value of ZnO NW-based triode under a V_g of 0 V is 3340. It is well known that the β value depends only on the geometry, structure, tip size and number of the emitters on the substrate, thus, the β value should be constant under various gate voltages. It is suggested that the observed large deviation from *F-N* fitting under a V_g of 10 V is attributed to that the gate trapping is the main mechanism at the gate leakage region.

The measurement of field emission properties of field emission triode based on low temperature synthesized ZnO NWs under a 30 W incandescent lamp irradiation with V_g of 20 V (operating in the gate controlled saturation region) was carried out to realize the influence of the illumination on the triode. As shown in Fig. 6.4 (a), the triode operating in the saturation region exhibits the typical field emission characteristics under the illumination. This *J-E* curve can also be divided into three

parts: zero emission (region 1 of Fig. 6.4 (a)), *F–N* field emission (region 2) and current saturation regions (region 3). The E_{on} and E_{th} decrease to 0.9 and 1.3 V/μm, respectively and the maximum current density increases to 2.5 A/cm^2 under the V_g of 20 V and E_a of 2.2 V/μm. The β value (3050) of illuminated ZnO NWs based field emission triode calculated from the slopes of the F–N plot (inset in the Fig. 6.4 (a)) is close to that of dark one. Therefore, it is demonstrated that the carriers in the ZnO NWs are excited during the illumination leading to increase the emission current density.

The J-V_g plots with various E_a of triode under a 30 W incandescent lamp irradiation are shown in Fig. 6.4(b). It is indicated that triode under such an illumination keeps the controllable behavior that could be separated into gate leakage region, linear region and saturation region. There is a large increase in the field emission current density under the optical illumination and the threshold gate bias of the triode operated under illumination is about 20 V. The average current density in the off region under the E_a of 2.2 V/μm is about 0.1 mA/cm^2, while that in the on region is about 0.5 A/cm^2. Thus, the triode performs the controllable field emission characteristics under the illumination, and the on/off current density ratio of this triode is about 5000 under the anode electric field of 2.2 V/μm. The inset in Fig. 6.4 (b) shows the relationships between g_m and V_g of the with E_a of 1.6 V/μm under the illumination, which exhibits a high g_m of 10 μS under the anode field of 1.6 V/μm and a gate bias of 20 V which is the optimized operation voltage of such a triode. Moreover, the μ value is about 200 under 2 mA/cm^2. Obviously, not only the emission current density was photoenhanced but the controllable ability is also enhanced under the optical illumination.

Figure 6.5 shows the field emission characteristics of the triode measured under the various pressures to realize the influence of measuring pressure on the

characteristics. This ZnO NWs based triode was swept from 0 to 2.2 V/μm with V_g of 0 V (avoiding the effects from the gate) under 1×10^{-6} Torr in the first 29 operations. In the first 29 tests, the field emission current densities are similar with the average current density of 2 mA/cm^2. Then, the following 2 sweeps were carried out under 1×10^{-3} Torr with Ar gas flowing in, and the current density is abruptly increased to 27 mA/cm^2. Finally, the pressure was decreased to 1×10^{-6} Torr again for the last 19 operations and the field emission current density remains in the average value of 27 mA/cm^2, which shows significant increase in comparison with that in the first 29 tests under the same measuring pressure. The field emission characteristics of the 1st and 50th sweeps of the triode are depicted in Fig. 6.5 (b), indicating that the E_{th} of 1st sweep is 2.1 V/μm while that of 50th sweep 1.6 V/μm. The calculated β value of 50th sweep of this triode device is 5203. Thus, such a triode exhibits the better emission properties, including the low turn-on and threshold electric fields, high emission current density and high β value after the measurement at high pressure of 1×10^{-3} Torr

The field emission ability and β value strongly depend upon the morphology of ZnO NWs. Figure 6.6 shows the FE-SEM image of the ZnO NWs after measuring in the high pressure and 50 times sweep, indicating that these ZnO NWs have smaller tips than the origin ones (Fig. 6.1(a)). It is suggested that these ZnO NWs measured in the high pressure were bombarded by argon ions leading to the formation of the smaller tips at the front of the NWs. Therefore, the observed improved emission properties of the triode are mainly due to such smaller tips of ZnO NWs. This result also provides a possible simple method to enhance the field emission properties of ZnO NWs based triode.

Based on the previous studies of our group[136], the vapor-liquid-solid (VLS) synthesized ZnO NWs with the higher aspect ratio and smaller tip diameter performed the better field emission characteristics (low threshold electric field, high current

density and high β value). However, those ZnO NWs applied in field emission devices are restricted to the high reaction temperature. In this article, the hydrothermal method provides a low temperature process to fabricate the ZnO NWs, which would be not only compatible with the Si-based microelectrics fabrication process but also possibly used in the polymer-based flexible electrooptical applications.

6.1.2 Conclusions

In this work, a field emission triode based on low temperature hydrothermally grown ZnO NWs was fabricated and characterized. The ZnO NWs based triode emitter was designed with a $100\times100\mu m^2$ cathode active region, which exhibits the gate controllable behavior and emits electrons at a threshold gate bias of 14 V with saturation current density of 12 mA/cm^2, g_m of 2.2 μS at a low operating E_a of 2.2 V/μm, and on-off ratio of up to 10^2. These controllable field emission properties of the triode can be enhanced under illumination. Moreover, the ZnO NWs based triode performs the better field emission properties after it was measured under high pressure leading to the formation of smaller tips of ZnO NWs. Our field emission triode with controllable transistor characteristics is expected to be appropriate for field emission display applications.

6.2 Under Gated Field Emission Triode

6.2.1 Structural and Electrical Analysis

The FE-SEM images of the fabricated ZnO based under gate structure are shown in the Figs. 6.7 (a), (b) and (c), indicating that the cathode active line is 10 μm in width, and the distance between the two active lines is 10 μm, respectively. The ZnO NWs are successfully and selectively grown on the ZnO seeding areas on the cathode metal regions, but no NWs and other impurities are grown on the gate metal regions. Figs. 6.7. (b) and (c) are the enlarged images of the under gate field emission device, the surface morphology of ZnO NWs on Al cathode metal can be classified into two morphology types: one type is the ZnO NWs that aggregate to form the flower-like secondary particles region and another is the few randomly distributed NWs grown on part of the cathode metal. Such a morphology variation is caused by the high lattice mismatch between Al (a = b = c = 4.05 Å) and ZnO (a = b = 3.25 Å, c= 5.21 Å). The lattice mismatch leads to be difficulty for the direct deposition of ZnO NWs on the Al cathode metal. Once ZnO grains are deposited on the substrate, the subsequent deposition of ZnO would be directed to the existing crystals. The type of nucleation results in forming the flower-like secondary particles. Thus, the ZnO NWs based under gate field emission device with the surface morphology of nonuniformity, random distribution and low number density. Based on the previous studies of our group[194], this flower-like ZnO NWs perform the better field emission characteristics (low threshold electric field, high current density and high β value) is suitable for field emission applications.

The relationship between emission current density (J) and applied anode electric field (E_a) of the ZnO NWs based under gate field emission triode for different gate bias (V_g) is shown in Fig. 6.8. As shown in the figure, the emission current density is

as small as the level of 10^{-7} A/cm^2 under the zero gate bias. While the V_g increases to 7.5 V, the electric threshold field (under current density of 1 mA/cm^2, E_{th}) is 1.5 V/μm but the J abruptly increases to 27 mA/cm^2 under E_a of 2.2 V/μm. Thus, the on/off current density ratio is up to 50000 under the anode electric field of 2.2 V/μm. The corresponding Fowler-Norheim (*F–N*) plots [$\ln(J/E_a^2)$ vs. E_a^{-1}] are depicted in the inset of Fig. 6.8, and the field enhancement factor, β, can be calculated from the slope of *F–N* plot by adopting the work function of ZnO (5.37 eV). As shown in the figure, the *F-N* plot under V_g of 7.5 V is obeying F-N relationship, and the calculated β value of ZnO NWs based under gate field emission device under a V_g of 7.5 V is 4551. Therefore, the field emission characteristics can be easily modulated by gate bias.

Figure 6.9 (a) shows the V_g dependence of J under various E_a of a under low temperature synthesis ZnO NW based gate field emission triode with 10 μm cathode width. As shown in the figure, the electron can't be emitted from ZnO NW emitters under the V_g of 0 V. The emission current started at a gate voltage of 6.0 V, and the anode current density abruptly increases to 27 mA/cm^2 under the anode electric field of 2.2 V/μm as the gate voltage was increased to 7.5 V. The linear intercept on V_g axis is the linear region threshold gate voltage, V_{gth}, and the threshold gate voltage of this under-gate field emission device is 6.5 V. The corresponding *F–N* plots ($\ln(I/V_g^2)$ vs. V_g^{-1}) are shown in the inset of Fig. 6.9, indicating that the field emission ability is obeying F-N relationship under the various anode bais. Like the gate bias increases, the anode electric field increases induce the change in the current density. Thus, the field emission under gate triode is not only the gate controllable but an anode controllable device.

The field emission characteristics also could be observed in the variation of small single transconductance (g_m) and amplification factor (μ). The inset in Fig. 6.9 (b) depicts the relationships between g_m and V_g of the ZnO NW-based under-gate field

emission triode. It is to be noted that the g_m is nearly zero below V_{gth} because the I_e is small at zero emission region. It goes through a maximum at the point of inflection of linear region in the I_a-V_g curve. The ZnO NW based under-gate field emission device exhibits a high g_m of 0.38 mS under the applied electric field of 2.2 V/μm and a low operating gate bias of 7.5 V which is the optimized operation of the field emission triode. From Fig. 6.9(a) $\mu \approx 400$ under the current density of 15 mA/cm^2 which is larger than that of planer triode based on low temperature ZnO NWs fabricated by our group[195] ($\mu \approx 100$). As the point of view, under gate field emission triode with the controllable ability is suitable for the FED applications.

6.2.2 Conclusions

In this study, an under-gate field emission device based on low temperature hydrothermally grown ZnO NWs was successfully fabricated. The ZnO NW based under-gate emitter was design with a 10 μm cathode active region in width. This device exhibits the gate controllable behavior and emits electrons with the V_{gth} of 7 V and the J up to 27 mA/cm^2 under the V_g of 7.5 V and E_a of 2.2 V/μm. The triode also displays a high g_m of 0.38 mS at a low operating E_a of 2.2 V/μm and V_g of 7.5 V. Thus, this insulator patterning under gate field emission triode with controllable characteristics is appropriate for field emission displays applications.

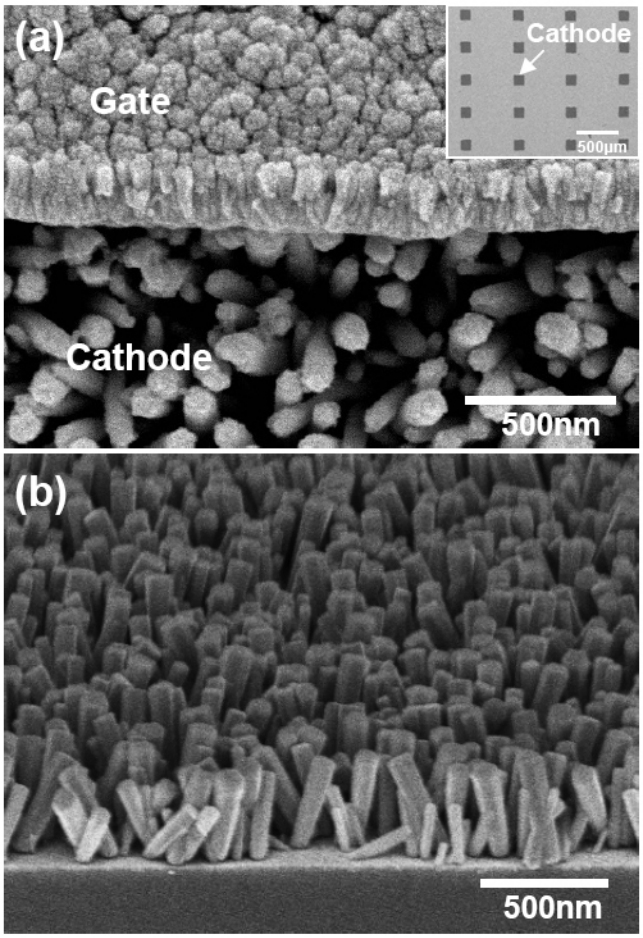

Figure 6.1 (a) FE–SEM micrographs of the triode near the gate edge. The inset is the 4×5 array triode with ZnO NWs islands grown inside gate holes. (b) Cross sectional FE–SEM image of ZnO NWs on the substrate.

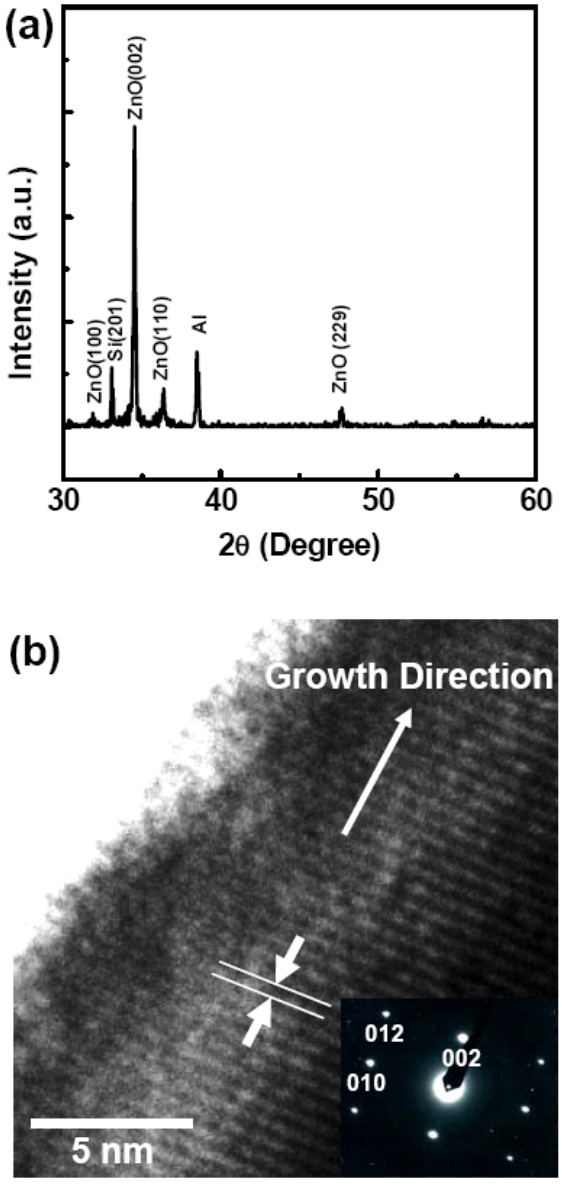

Figure 6.2 (a) XRD pattern of ZnO NWs triode. (b) HRTEM micrograph of ZnO NWs, and the inset is the corresponding SAED of the NWs.

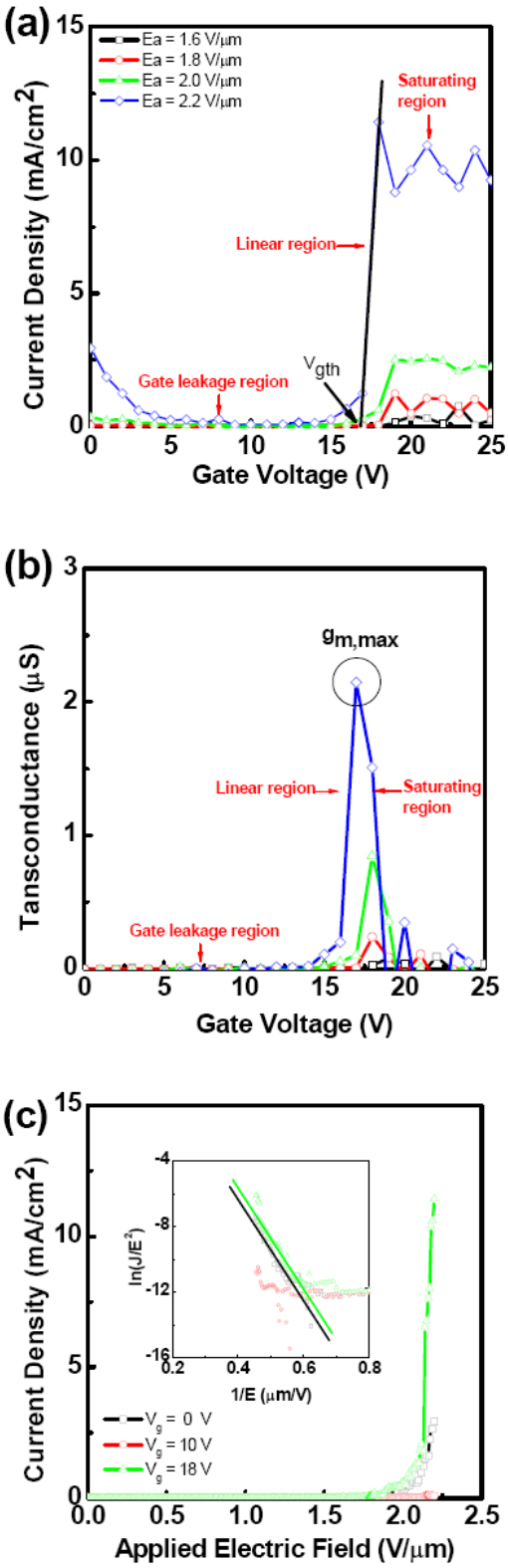

Figure 6.3 (a) Field emission current density versus gate voltage (J–V_g) curves under the various applied electric field. (b) Relation of transconductance versus gate voltage of the field emission triode. (c) Field emission current density versus applied electric field curves under the gate voltage of 0, 10 and 18V, respectively. The inset is the corresponding Fowler–Nordheim plots.

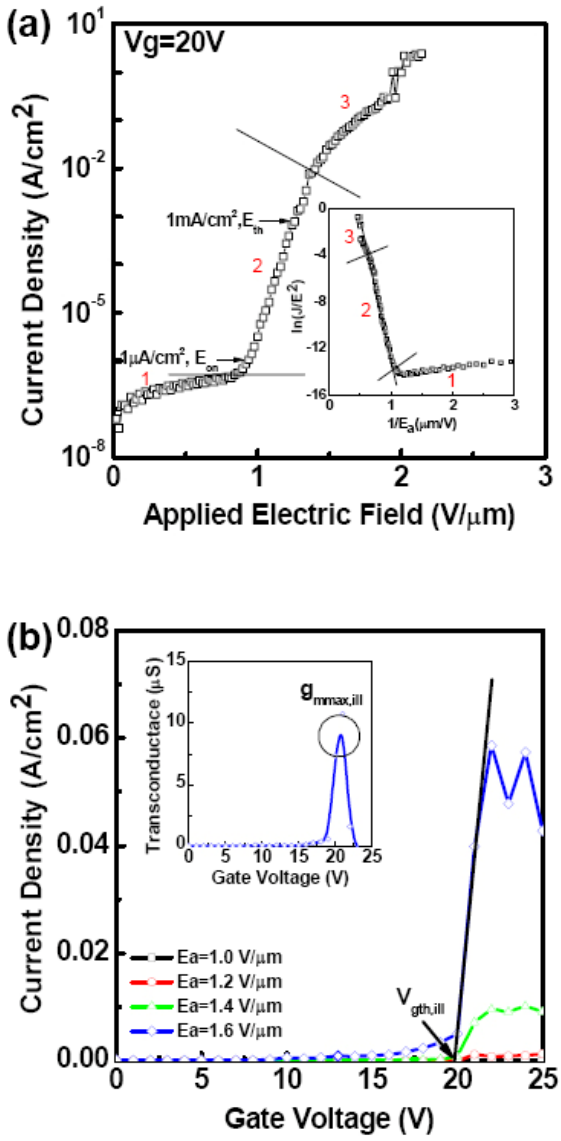

Figure 6.4 (a) Photoenhanced field emission characteristics of ZnO NWs triode device operating at 20 V of V_g. The insert is the corresponding F–N plots. (b) Photoenhanced field emission current density versus gate voltage (J–V_g) curves under the various applied electric field, and the insert is the gm vs. V_g under E_a of 2.2 V/μm.

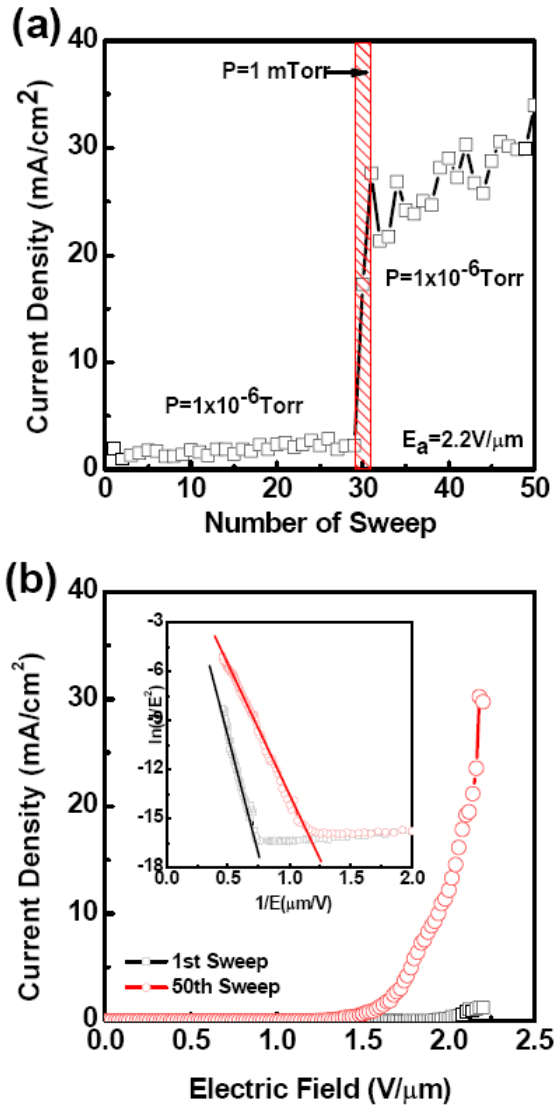

Figure 6.5 (a) The emission current density of ZnO NWs based field emission triode under various pressures. (b) The 1st and 50th sweep of *J*-E_a curves and the corresponding *F*-*N* plots.

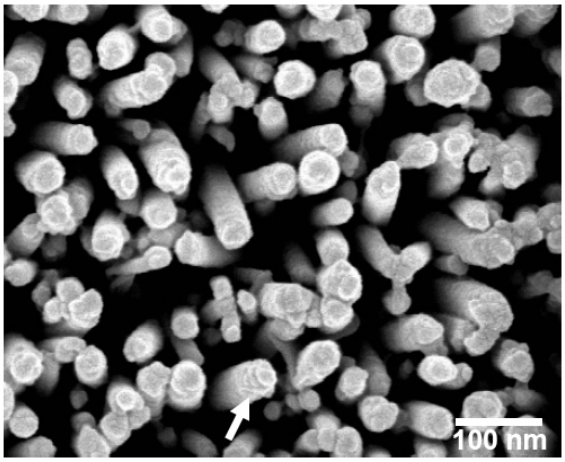

Figure 6.6 FE-SEM images of ZnO NWs after 50th *J*-E_a sweeps.

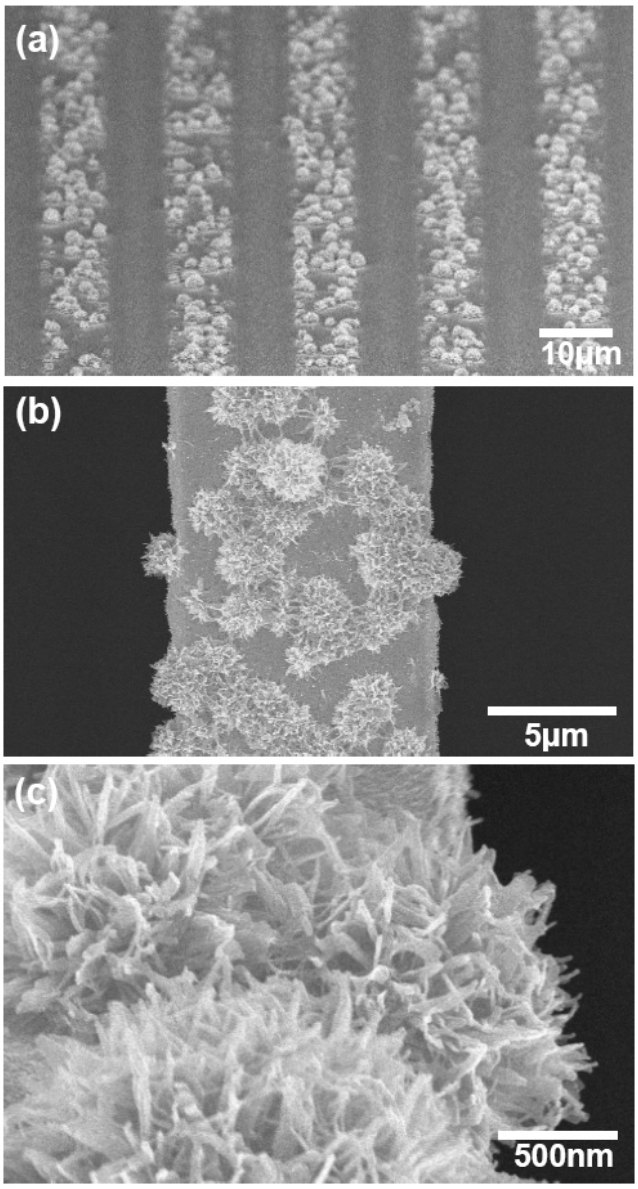

Figure 6.7 FE–SEM micrographs of the under-gate field emission triode.

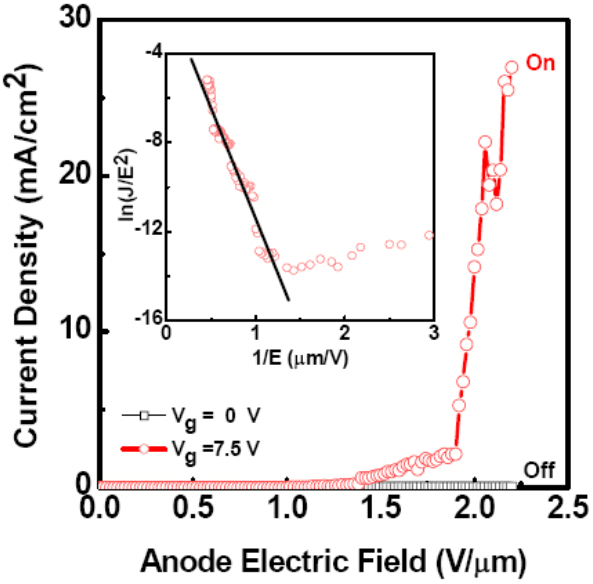

Figure 6.8 Field emission current density versus applied electric field curves under the gate voltage of 0 and 7.5V, respectively. The inset is the corresponding Fowler–Nordheim plot under gate voltage of 7.5V.

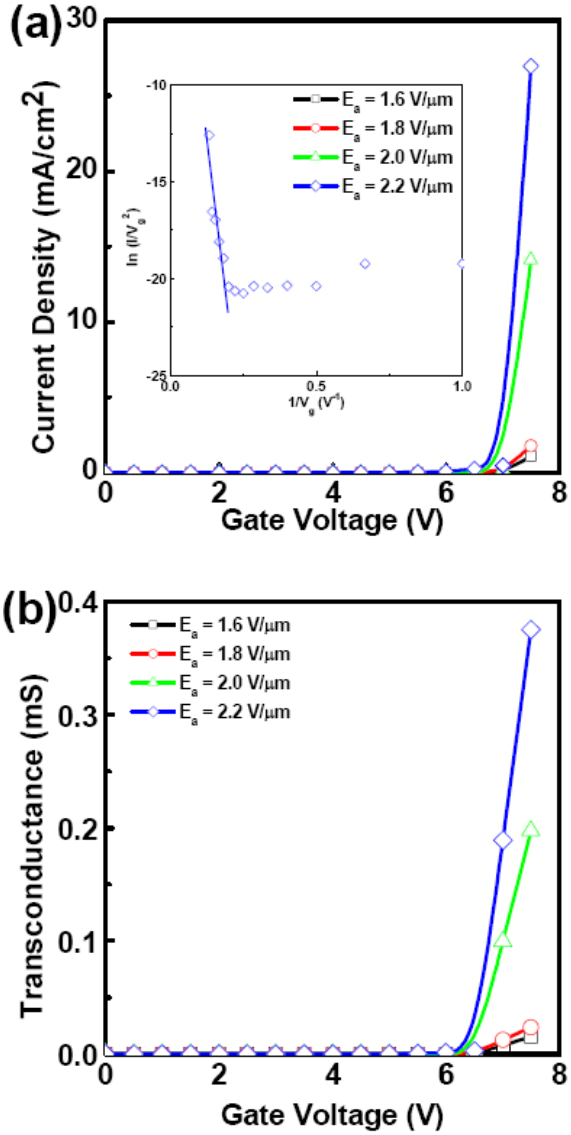

Figure 6.9 (a) Field emission current density versus gate voltage curves under the various anode electric fields. The inset is the corresponding F-N plot under anode electric field of 2.2 V/μm. (b) The relation of transconductance versus gate voltage of the under-gate field emission device.